Simulation and Surface Topology of Activity of Pyrazoloquinoline Derivatives as Corrosion Inhibitor on the Copper Surfaces

Razieh Razavi (r.razavi@ujiroft.ac.ir)
university of jiroft
Mahboobeh Zahedifar
university of jiroft
Sayed Ali Ahmadi
azad university of kerman

Research Article

Keywords: copper, inhibitor, pyrazole, simulation

Posted Date: February 17th, 2021

DOI: https://doi.org/10.21203/rs.3.rs-199588/v1

Abstract

In the present study, interactions of pyrazolo [3,4-b]quinoline-3,5-dione derivatives on copper metal surface were considered using B3LYP/6-311 + + g(d,p) in water media and also interaction energies were simulated for all the chemical coordination's of pyrazoloquinoline derivatives compounds. Moreover the original and novel results revealed that in all the chemical side effects and cases, pyrazoloquinoline derivatives compounds were located on the Cu metal surface. This shows that the most important desired direction is where the concentrated numbers of electron donor active atoms of inhibitor molecules interacted with the Cu metal surface atom. Furthermore the chemical Thermodynamic parameters were estimated for example: ΔG of chemical inhibitor complexes with the Cu metal surface. Density of the electron profile analysis and chemical electrostatic potential of nuclear charges in the molecule were applied to consider the nature of a number of probable interactions between Cu metal surface and inhibitors in terms of bond critical point (BCP). Finally chemical electronics parameters showed that the OH and NO_2 pyrazoloquinoline derivatives have best interaction in chemical and surface media.

Introduction

The heterocyclic compounds containing pyrazole and quinoline systems, such as pyrazolo[1,5-]pyrimidine, pyrazolopyridine, pyrazoloquinolone, pyrazolo[4,3-c]quinoline and pyrazolo[1,5]quinazoline play an important role in drug development and chemistry of medicine. Pyrazolo[3,4- b]quinoline frame offers important antiviral, antimalarial, and anti-inflammatory activity [1] and also corrosion activity[2]. In other words, given the double bond and heteroatoms in quinoline and pyrazole, corrosion inhibition effects of surface atom on metal [3–10] have been investigated previously. Corrosion inhibition effect strongly depends on adsorption on the surface of metal. It has been shown that corrosion inhibition is influenced by different factors like type of corrosive material, chemical essence of the metal ,and structure of the chemical component applied as active inhibitor that is directly associated with adsorption capability at the alloy and metal atom on surface [11]. Simulation of molecular modeling and progression of quantum chemical kinetics have led to combination of efficiency with chemical and electronic molecular properties[12, 13, 22–31, 14, 32, 15–21].

Therefore, in this theoretical study, corrosion inhibition activity of pyrazolo[3,4-b]quinoline-3,5-dione derivatives (R = Ph, 2-$(NO_2)C_6H_4$, 4-(N,N-di-Me)C_6H_4, 2,4-di-ClC_6H_3, 2-$(OH)C_6H_4$, 4-$(OH)C_6H_4$, 4-$(Me)C_6H_4$, 4-$(OCH_3)C_6H_4$, 4-$(Cl)C_6H_4$) on Cu surface was investigated, and interaction of the Cu atom surface with adsorption energies and also topologies of the molecular structure were obtained and evaluated. Charge densities due to adsorption reaction were calculated. The interface was created for simulation of molecule/metal surface. Reactivity of Cu surface with the molecule was also estimated.

Computational Method

Optimized geometries were done by B3LYP/6-311G++(d,p) level as employed in the Gaussian 09 program[33]. Topological study on the surface density of electron at density functional theory(DFT) optimization of chemical structures in complexes between Cu atom surface and pyrazoloquinoline molecule derivatives (R = Ph, 2-$(NO_2)C_6H_4$, 4-(N,N-di-Me)C_6H_4, 2,4-di-ClC_6H_3, 2-$(OH)C_6H_4$, 4-$(OH)C_6H_4$, 4-$(Me)C_6H_4$, 4-$(OCH_3)C_6H_4$, 4-$(Cl)C_6H_4$) was done using the quantum theory of atoms in molecules. Stoichiometric ratio of 1:1 was considered for complexes of Cu surface- pyrazolo [3,4-b]quinoline-3,5-dione derivatives .

Concisely, the inhibitors were simulated on the Cu surface in all directions. Virial theorem was applied to investigate the BCPs. The characteristics including density of electron (ρ) and ($\nabla^2\rho$) were measured at BCP. Highest occupied molecular orbital and lowest unoccupied molecular orbital were accomplished on the planned chemical system. Physical chemistry characteristics, for example dipole moment, η, and μ of the desired chemical molecules were studied. Thermal energies were computed by frequencies. Differences in the Gibbs free energies between the pyrazoloquinoline derivatives, and Cu surface with pyrazoloquinoline derivatives were used to estimate the Gibbs free formation energy of compounds in water at T = 298.15 K. The polarizable continuum model (PCM) was employed for solvent effects.

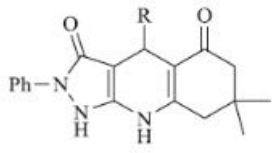

R = Ph, 2-(NO_2)C_6H_4, 4-(N,N-di-Me)C_6H_4, 2,4-di-ClC_6H_3, 2-(OH)C_6H_4, 4-(OH)C_6H_4, 4-(Me)C_6H_4, 4-(OCH_3)C_6H_4, 4-(Cl)C_6H_4

Results And Discussion

The important goal of this research is illustrating structural and electronic interactions between Cu(fcc) surface with various orientations of pyrazoloquinoline derivatives (R = Ph, 2-(NO_2)C_6H_4, 4-(N,N-di-Me)C_6H_4, 2,4-di-ClC_6H_3, 2-(OH)C_6H_4, 4-(OH)C_6H_4, 4-(Me)C_6H_4, 4-(OCH_3)C_6H_4, 4-(Cl)C_6H_4) as inhibitors. Electrochemical and thermodynamic principles are the original principles of corrosion behavior defining transformation of the alloys and metals into stable states. Figures 1 and 2 show all the optimized desired structures. Nitrogen and oxygen heteroatoms in pyrazoloquinoline molecule could interact with the Cu surface. Also, electrons of benzene ring on R derivatives interacted with surface atom of the metal compound in parallel and perpendicular orientations. All the parallel and perpendiculars orientations were simulated for chemical inhibitor molecules as exemplified in Fig. 4. Table 1 shows the exchanges of Gibbs free energy of Cu complexes with the chemical inhibitor pyrazoloquinoline molecule derivatives. Optimized sides of the inhibitor molecules are perpendicular to interact with Cu surface. Pyrazole ring has an effective side in the interaction field at Cu complexes. Thermodynamics leads spontaneous direction of the reaction and is applied to investigate and estimate whether corrosion behavior on metal surfaces is probable or not theoretically. According to the results presented in Table 1, all the Cu complexes had negative Gibbs free energy showing that all the derivatives can participate in spontaneous reaction. Figure 3 and Table 2 illustrate different ranges of energy in pyrazoloquinoline derivatives and Cu complexes of pyrazoloquinoline derivatives.-NO_2 and -OH functions had the minimum negative value of Gibbs free energy and they had a strong interaction among the other pyrazoloquinoline derivatives. Figure 3 illustrates the pyrazoloquinoline derivative inhibitors with electron-rich groups. Spatial congestion may cause –NO2 and –OH to have minimum Gibbs free energy leading to the best stability in water phase.

Table 1
Gibbs free energy of Cu and of pyrazoloquinolines derivatives' structure (R = Ph, 2-(NO2)C6H4, 4-(N,N-di-Me)C6H4, 2,4-di-ClC6H3, 2-(OH)C6H4, 4-(OH)C6H4, 4-(Me)C6H4, 4-(OCH3)C6H4, 4-(Cl)C6H4) and Cu complexes

Cu/R Complexes	Ph	2-(NO2)C6H4	4-(N,N-di-Me)C6H4	2,4-di-ClC6H3	2-(OH)C6H4	4-(OH)C6H4	4-(Me)C6H4	4-(OCH3)C6H4	4-(Cl)C6H4
ΔG/ Kcal/mol	-4.87	-5.17	-4.82	-4.72	-5.35	-5.06	-4.41	-4.96	-4.76

Table 2
Gibbs free energy

R/Compunds	Δ*G* (cal/mol)	HOMO (a.u.)	LUMO (a.u.)
Ph	-780.37	-0.22198	-0.06357
2-(NO_2)C_6H_4	-908.2	-0.2136	-0.155798
4-(N,N-di-Me)C_6H_4	-863.99	-0.16813	-0.05483
2,4-di-ClC_6H_3	-1356.75	-0.21018	-0.05595
2-(OH)C_6H_4	-827.14	-0.21086	-0.05429
4-(OH)C_6H_4	-827.14	-0.21137	-0.05684
4-(Me)C_6H_4	-804.62	-0.20843	-0.05402
4-(OCH_3)C_6H_4	-851.79	-0.2117	-0.05726
4-(Cl)C_6H_4	-1068.32	-0.20883	-0.05656

Essentially, corrosion consists of two half-cell electrochemical reactions. Anodic and cathodic reactions involve leaving and taking up of the unrestricted and free electron by ionization of the metal or alloys nevertheless, cathodic reaction implicates taking up of free electrons by the dissolved oxygen in electrolyte molecules. On the oxidation reaction and solution reaction, free electrons are shaped although reduction reaction occurs later in which the electrons have been accepted. Corrosion behavior of metals and alloys can simply control the use of the electrochemical principles[34]. Corrosion inhibition properties of the alloys and metals can change because of adsorption of chemical inhibitor at solution/ metal interface significantly. Inhibition action of surface corrosion occurs at surface that includes electron transformation and adsorption of chemical inhibitors on the metal atom surface in electrolyte. DFT essences on electron density (ρ) [35] take place relatively for each electron, in place of the carrier of whole data underground state of molecule formation, as an electron wave function.

For recognizing electron donating and electron accepting roles of pyrazolo[3,4-b]quinoline-3,5-dione derivatives (R = Ph, 2-(NO_2)C_6H_4, 4-(N,N-di-Me)C_6H_4, 2,4-di-ClC_6H_3, 2-(OH)C_6H_4, 4-(OH)C_6H_4, 4-(Me)C_6H_4, 4-(OCH3)C_6H_4, 4-(Cl)C_6H_4), HOMO and LUMO energies of them were calculated theoretically as shown in Table 2.

Table 3
Quantum descriptor of pyrazoloquinolines derivatives

R-Compounds	*IP*(eV)	*EA*(eV)	χ(eV)	η(eV)	μ(eV)	Dipole moment(Debye)
Ph	3.6	1.04	2.32	1.28	-2.32	8.44
2-(NO_2)C_6H_4	3.5	2.5	3	0.5	-3	5.79
4-(N,N-di-Me)C_6H_4	2.7	0.89	1.79	0.9	-1.79	8.92
2,4-di-ClC_6H_3	3.44	0.91	2.17	1.26	-2.17	7.94
2-(OH)C_6H_4	3.45	0.88	2.16	1.28	-2.16	9.62
4-(OH)C_6H_4	3.46	0.93	2.19	1.26	-2.19	9.47
4-(Me)C_6H_4	3.41	0.885	2.14	1.262	-2.14	8.91
4-(OCH_3)C_6H_4	3.47	0.93	2.2	1.27	-2.2	10.66
4-(Cl)C_6H_4	3.42	0.92	2.17	1.25	-2.17	9.48

Table 4
Topological parameters of pyrazoloquinolines derivatives

R-Complexes	BCP	ρ	∇^2ρ
	a	0.2644	-0.79
	b	0.2635	-0.783
	c	0.2639	-0.787
2-(NO_2)C_6H_4	a	0.2202	-0.3293
	b	0.3194	$-0.7386*10^{-1}$
	c	0.3198	$-0.7501*10^{-1}$
4-(N,N-di-Me)C_6H_4	a	0.2422	-0.5169
	b	0.2352	-0.4886
	c	0.2719	-0.8282
2,4-di-ClC_6H_3	a	0.2957	-0.6874
	b	$0.1849*10^{-1}$	$-0.7447*10^{-1}$
	c	0.1669	-0.1449
2-(OH)C_6H_4	a	0.2340	-0.85
	b	$0.2369*10^{-2}$	+ 0.66
	c	0.3427	-0.42
4-(OH)C_6H_4	a	0.4364	-0.8739
	b	$0.2911*10^{+3}$	-0.4015
	c	0.4157	-0.1654*10
4-(Me)C_6H_4	a	0.2689	-0.8028
	b	0.2681	-0.8028
	c	0.2688	-0.7975
4-(OCH_3)C_6H_4	a	0.1879	-0.2055
	b	0.2267	-0.2934
	c	0.2760	-0.8688
4-(Cl)C_6H_4	a	0.2722	-0.8442
	b	0.2748	-0.8748
	c	0.3190	-0.8185

DFT is an easy technique to consider chemical molecular structure and activities of corrosion inhibitors[10][36][37] on surface. Simulation has been developed as a powerful tool to scrutinize metal complex atom of corrosion surface [38]. Mechanism of corrosion was detected by checking electron distribution Fig. 5 and Fig. 6 and molecular adsorption on metal and metal oxide surfaces.

Set orbit of linear combinations of geosynchronous functions was used for the basis aimed at electronically computing the design. Linear combination of several codgers was used due to accurate representation of atomic orbitals.

Definition of HOMO and LUMO orbital energy levels of chemical molecules is significant. Fukui [39] acknowledged that frontier orbitals are important because stereochemistry of the inhibitor coordination and stereochemistry ratio of the components in

reactions are the original characteristics leading to reaction simplicity. E_{HOMO} and corrosion resistance have a good relationship that is obtained by potential of the chemical compounds, which is important as inhibitor adsorption on the metal surface atom is the source of giving electron on chemical interaction of heteroatom electrons and π electrons of benzene ring with empty d orbitals of metal surface atoms [40]. Possibly, numerous levels of E_{HOMO} are required to specify tendency of electron donating in the chemical compounds to the empty acceptor atom orbitals of chemical compounds where the electron accepting capacity of the molecules is determined by energy of the lower empty orbitals. As indicated in Table 2, –Ph, -OMe, -NO_2, and –OH had π electron and heteroatoms and high HOMO energy to donate electron to the Cu surface. –Ph π electron caused maximum donating level of energy. Considerable inhibition efficiency has been provided by low tenets of difference in energy, because orbital of the metal surface has less contribution correctly for decreasing the energy from occupied orbital of atoms that is obtained in the previous energy level[41].

The μ of chemical molecules is a trajectory value that is most widely applied for reporting polarization of a chemical molecule. It shows the amount of departure of the two electrical charges (negative and positive). The μ is useful for scattering of the electrons among the two bonded chemical atoms. Actually, according to μ, the change in polar and non-polar chemical bonds is different. In the pure dipole moment, the molecule is actually small or zero thus, molecular bonding and molecules are deliberately non-polar and polar molecules, respectively by pure bipolar moment. According to the results presented in Table 3, -OMe and –OH functions had the biggest dipole moment that showed most polarity in chemical solutions. It means that the chemical bonds had non-similar electronegativity. Similar electronegativity of atom values produces the chemical bonds by exact smaller dipole moment. Total dipole moment, on the other hand, reproduces just the global injunction of polarization in a chemical molecule rather than a single bond notification so that, efficiency of inhibitor diminishes by decreasing efficiency. Therefore, -OH and -OMe groups act as the best inhibitor on Cu surface [42]. Positive signs of numbers of dipole moment indicate that the inhibitors could be applied to the metal surface by physical mechanism [43]. All the pyrazoloquinoline derivatives have positive dipole moment so they have physical mechanism of inhibition. DFT effectively recognizes chemical selectivity and reactivity ,according to quantum molecular properties, like chemical potential (μ) and electronegativity(χ) [44]. Another chemical parameter is the total hardness (η), which analyzes molecular selectivity and selectivity of reaction. Relationship between corrosion inhibition and quantum chemical quantities was established by the Pearson's and Lewiss theory of hard and soft acids and bases. Accordingly, a hard molecule has a high level of gap energy indicating hard natural surroundings of compounds, and a soft chemical molecule has a low level of band gap energy. Due to low band gap energy level, electrons could be provided to acceptor atom from soft compound in comparison with hard compound easily. Therefore, the reactive site is where the molecule is absorbed by the highest level of energy[45]. Table 3 shows all the results related to the pyrazolo [3,4-b]quinoline-3,5-dione derivatives. –OH, -OMe, and –NO_2 had large value of hardness therefore, they were more reactive among the other pyrazoloquinoline derivatives. Chemical interactions of molecules are also covalent and/or polar electrostatically. Charge of electric force field in compounds is responsible for chemical electrostatic interactions obviously. Biological behavior of the molecules results from native electron density and/or charge of atom, which are significant for making properties of all the chemical and physico-chemical reactions. Figures 4 5 show the profile of charge density of pyrazoloquinoline derivatives and profile of electrostatic potential from nuclear charges in Cu complexes of pyrazoloquinoline derivatives. Molecular polarization is described by atomic charge of the molecules. Increase in the electron discharging power was exchanged by electron-donating molecules like (-OCH_3 and –OH group) that occurred to improve prohibition but, electron-attracting group (-Cl) in pyrazoloquinoline derivatives decreases the effect of prohibition. There are two important quantum functions including electron-localization function and Laplacian density of electron exposing the electron donations linked with the amount of spatial structure arrangement of pairs in the localized electron implicitly in quantum model of VSEPR. Consequently, interpretation of both experimental and theoretical electron densities was used. Potential local energies and electronic kinetic were used for training the bonding in chemical compounds and lattices of metal crystals [46]. The power of bonding was determined by topological parameters Fig. 6. There are numerous geometrical principles for determining the distance of bonds between Cu atom surface and chemical inhibitor molecules [30]. The QTAIM was established by electron density (ρ) related to attendance of (3,-1) and (+ 3,-3) BCPs for the proton inhibitors principally. Acceptor atom of Cu surface interaction validates bonding interaction and the range of electron density is from 0.002 to 0.04 a.u. Laplacian corresponding density must be equal to 0.024–0.139 a.u. Table 4 presents the results regarding calculating the topological factors of the desired bonds like $\nabla^2\rho$ and ρ. Value of + 0.66 for –OH group in the pyrazolo [3,4-b]quinoline-3,5-dione derivatives showed active BCP for making reaction.

Conclusion

Defined calculation data were provided by B3LYP/6-311 + + g(d,p). Formation of the complexes of pyrazolo [3,4-b]quinoline-3,5-dione derivatives with Cu (fcc) surface atom was studied by the mentioned procedures. Due to energies of interaction and simulation sides of reaction, inhibitor molecules were placed in perpendicular orientation with the Cu surface. Heavy relations were between O, and N heteroatoms of inhibitors and π electron in benzene rings with Cu atoms. QTAIM indicators were simulated as quantitative proof to understand the environment of bond interactions between Cu surfaces and the chemical inhibitors. Results of the QTAIM simulation showed the popular interactions formed between Cu surface and inhibitors by –OH group of pyrazoloquinoline derivatives. Dipole moments depicted that polarity and solubility of the chemical complexes increase by adding chemical inhibitors to the Cu surface. Theoretical calculations supported that –OH and -OMe group functions act as the best inhibitor for Cu surface.

Declarations

Funding: This study was supported by University of Jiroft without paying Grants.

Conflict of Interest: The authors declare that they have no conflict of interest.

References

1. M. Zahedifar, R. Shojaei, and H. Sheibani, Res. Chem. Intermed. **44**, 873 (2018).
2. L. O. Olasunkanmi, I. B. Obot, and E. E. Ebenso, RSC Adv. **6**, 86782 (2016).
3. A. M. Eid, S. Shaaban, and K. Shalabi, J. Mol. Liq. **298**, 111980 (2020).
4. H. Rahmani, K. I. Alaoui, M. EL Azzouzi, F. Benhiba, A. El Hallaoui, Z. Rais, M. Taleb, A. Saady, B. Labriti, A. Aouniti, and A. Zarrouk, Chem. Data Collect. **24**, 100302 (2019).
5. L. H. Madkour, S. Kaya, and I. B. Obot, J. Mol. Liq. **260**, 351 (2018).
6. R. Farahati, A. Ghaffarinejad, S. M. Mousavi-Khoshdel, J. Rezania, H. Behzadi, and A. Shockravi, Prog. Org. Coatings **132**, 417 (2019).
7. R. Farahati, H. Behzadi, S. M. Mousavi-Khoshdel, and A. Ghaffarinejad, J. Mol. Struct. **1205**, 127658 (2020).
8. E. Kamali Ardakani, E. Kowsari, and A. Ehsani, Colloids Surfaces A Physicochem. Eng. Asp. **586**, 124195 (2020).
9. Z. Iqbal, Z. Ashraf, M. Hassan, Q. Abbas, and E. Jabeen, Bioorg. Chem. **90**, 103108 (2019).
10. B. El Ibrahimi, A. Soumoue, A. Jmiai, H. Bourzi, R. Oukhrib, K. El Mouaden, S. El Issami, and L. Bazzi, J. Mol. Struct. **1125**, 93 (2016).
11. L. Zeidabadinejad, 1715 (2019).
12. B. Tan, S. Zhang, Y. Qiang, L. Guo, L. Feng, C. Liao, Y. Xu, and S. Chen, J. Colloid Interface Sci. **526**, 268 (2018).
13. B. Tan, S. Zhang, Y. Qiang, W. Li, H. Li, L. Feng, L. Guo, C. Xu, S. Chen, and G. Zhang, J. Mol. Liq. **298**, 111975 (2020).
14. K. O. Sulaiman, A. T. Onawole, O. Faye, and D. T. Shuaib, J. Mol. Liq. **279**, 342 (2019).
15. A. S. Fouda, M. A. Ismail, A. A. Al-Khamri, and A. S. Abousalem, J. Mol. Liq. **290**, 111178 (2019).
16. M. Abdallah, E. A. M. Gad, M. Sobhi, J. H. Al-Fahemi, and M. M. Alfakeer, Egypt. J. Pet. **28**, 173 (2019).
17. A. Dehghani, G. Bahlakeh, B. Ramezanzadeh, and M. Ramezanzadeh, Constr. Build. Mater. **245**, 118464 (2020).
18. G. Bahlakeh, B. Ramezanzadeh, A. Dehghani, and M. Ramezanzadeh, J. Mol. Liq. **283**, 174 (2019).
19. R. Hsissou, S. Abbout, R. Seghiri, M. Rehioui, A. Berisha, H. Erramli, M. Assouag, and A. Elharfi, J. Mater. Res. Technol. 1 (2020).
20. R. Hsissou, F. Benhiba, S. Abbout, O. Dagdag, and S. Benkhaya, Inorg. Chem. Commun. **115**, 107858 (2020).
21. R. Hsissou, O. Dagdag, S. Abbout, F. Benhiba, M. Berradi, M. El Bouchti, A. Berisha, N. Hajjaji, and A. Elharfi, J. Mol. Liq. **284**, 182 (2019).
22. K. Cherrak, F. Benhiba, N. K. Sebbar, E. M. Essassi, M. Taleb, A. Zarrouk, and A. Dafali, Chem. Data Collect. **22**, 100252 (2019).
23. V. Sok and A. Fragoso, Int. J. Biol. Macromol. **118**, 427 (2018).
24. T. T. Adebesin, N. W. Odozi, I. A. Oladosu, and T. I. Odiaka, Inorg. Chem. Commun. **107**, 107501 (2019).
25. G. Chen, T. Wenga, W. Ma, and F. Lin, Appl. Energy **247**, 630 (2019).

26. Z. Rouifi, F. Benhiba, M. El Faydy, T. Laabaissi, H. About, H. Oudda, I. Warad, A. Guenbour, B. Lakhrissi, and A. Zarrouk, Chem. Data Collect. **22**, 100242 (2019).
27. M. Ouakki, M. Galai, M. Rbaa, A. S. Abousalem, B. Lakhrissi, E. H. Rifi, and M. Cherkaoui, Heliyon **5**, (2019).
28. Z. Sanaei, G. Bahlakeh, B. Ramezanzadeh, and M. Ramezanzadeh, J. Mol. Liq. **290**, 111176 (2019).
29. J. Aslam, R. Aslam, I. Hussain, and N. R. E. Radwan, Integr. Med. Res. 1 (2020).
30. I, C. Yu, R. Chen, J. J. Li, J. J. Li, M. Drahansky, M. . Paridah, A. Moradbak, A. . Mohamed, H. abdulwahab taiwo Owolabi, FolaLi, M. Asniza, S. H. . Abdul Khalid, T. Sharma, N. Dohare, M. Kumari, U. K. Singh, A. B. Khan, M. S. Borse, R. Patel, A. Paez, A. Howe, D. Goldschmidt, C. Corporation, J. Coates, and F. Reading, Intech **i**, 13 (2012).
31. M. Mihit, K. Laarej, H. Abou El Makarim, L. Bazzi, R. Salghi, and B. Hammouti, Arab. J. Chem. **3**, 55 (2010).
32. G. L. F. Mendonça, S. N. Costa, V. N. Freire, P. N. S. Casciano, A. N. Correia, and P. de Lima-Neto, Corros. Sci. **115**, 41 (2017).
33. G. E. S. M. J. Frisch, G. W. Trucks, H. B. Schlegel, B. M. M. A. Robb, J. R. Cheeseman, G. Scalmani, V. Barone, H. P. H. G. A. Petersson, H. Nakatsuji, M. Caricato, X. Li, M. H. A. F. Izmaylov, J. Bloino, G. Zheng, J. L. Sonnenberg, T. N. M. Ehara, K. Toyota, R. Fukuda, J. Hasegawa, M. Ishida, J. Y. Honda, O. Kitao, H. Nakai, T. Vreven, J. A. Montgomery, E. B. J. E. Peralta, F. Ogliaro, M. Bearpark, J. J. Heyd, J. N. K. N. Kudin, V. N. Staroverov, R. Kobayashi, J. T. K. Raghavachari, A. Rendell, J. C. Burant, S. S. Iyengar, J. B. C. M. Cossi, N. Rega, J. M. Millam, M. Klene, J. E. Knox, R. E. S. V. Bakken, C. Adamo, J. Jaramillo, R. Gomperts, J. W. O. O. Yazyev, A. J. Austin, R. Cammi, C. Pomelli, G. A. V. R. L. Martin, K. Morokuma, V. G. Zakrzewski, A. D. D. P. Salvador, J. J. Dannenberg, S. Dapprich, J. C. O. Farkas, J. B. Foresman, J. V. Ortiz, and and D. J. Fox, (n.d.).
34. S. K. Saha, A. Dutta, P. Ghosh, D. Sukul, and P. Banerjee, Phys. Chem. Chem. Phys. **17**, 5679 (2015).
35. T. Lu and F. Chen, J. Comput. Chem. **33**, 580 (2012).
36. Y. Liu, Y. Peng, B. An, L. Li, and Y. Liu, Chemosphere **246**, 125778 (2020).
37. a Balakrishnan, … Adv. Sci. … **1**, 19 (2012).
38. K. F. Khaled and M. A. Amin, Corros. Sci. **51**, 2098 (2009).
39. K. Fukui, Science (80-.). **218**, 747 (1982).
40. N. Khalil, Electrochim. Acta **48**, 2635 (2003).
41. M. El Faydy, B. Lakhrissi, C. Jama, A. Zarrouk, L. O. Olasunkanmi, E. E. Ebenso, and F. Bentiss, J. Mater. Res. Technol. **9**, 727 (2019).
42. G. Gao and C. Liang, Electrochim. Acta **52**, 4554 (2007).
43. M. Bouklah, N. Benchat, A. Aouniti, B. Hammouti, M. Benkaddour, M. Lagrenée, H. Vezin, and F. Bentiss, Prog. Org. Coatings **51**, 118 (2004).
44. L. H. Mendoza-Huizar and C. H. Rios-Reyes, J. Mex. Chem. Soc. **55**, 142 (2011).
45. X. Xu, W. Xing, Y. Chen, F. Liu, X. Wu, T. Dong, P. Ye, Z. Liu, and H. Huang, Synth. Met. **231**, 19 (2017).
46. V. Tsirelson and A. Stash, Acta Crystallogr. Sect. B Struct. Sci. **58**, 780 (2002).

Figures

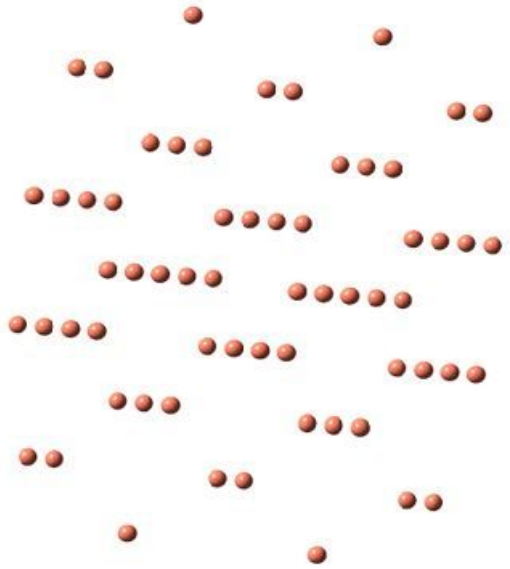

Figure 1

Optimized Cu (fcc) structure

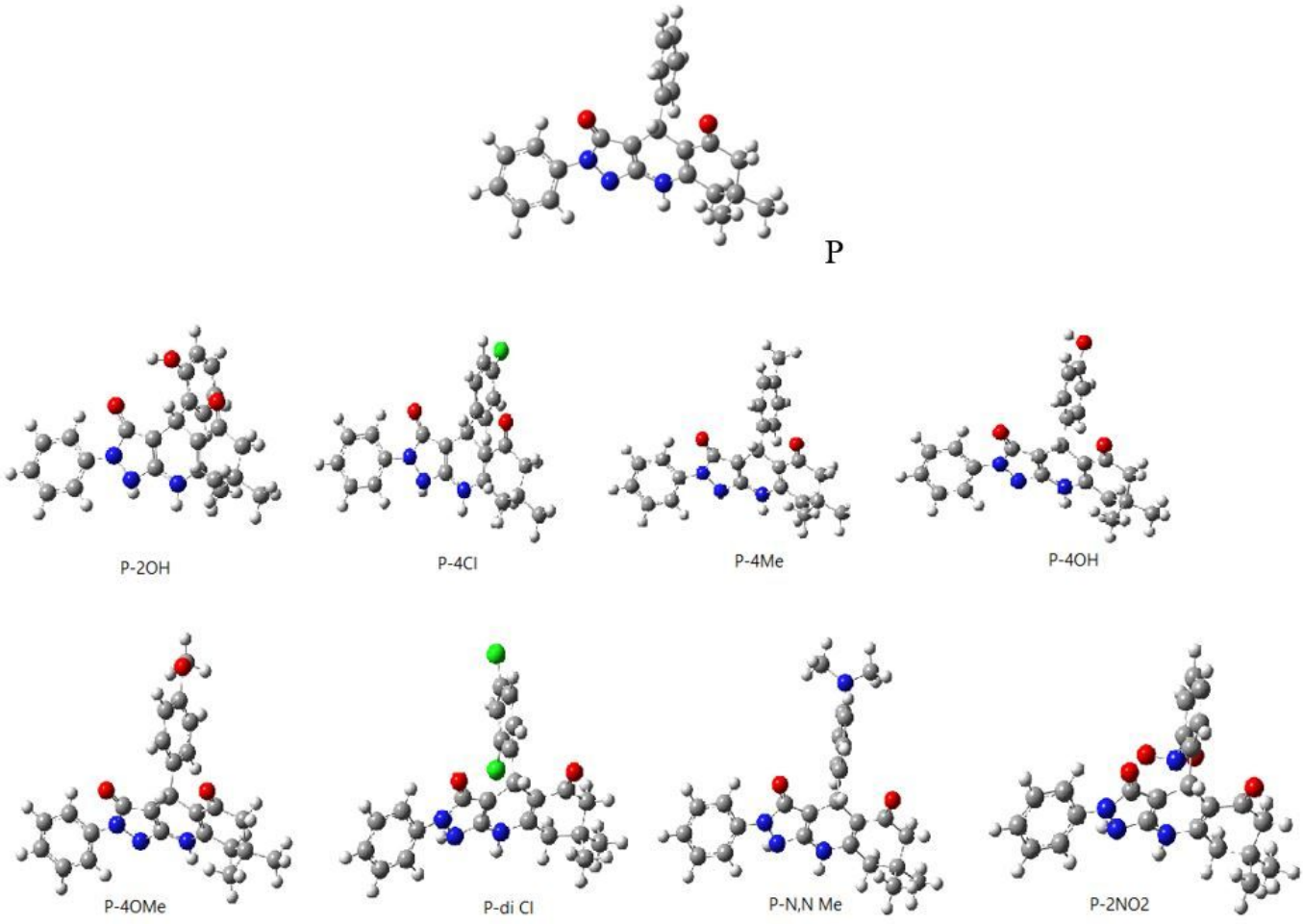

Figure 2

Optimized pyrazoloquinolines derivatives' structure (R= Ph, 2-(NO2)C6H4, 4-(N,N-di-Me)C6H4, 2,4-di-ClC6H3, 2-(OH)C6H4, 4-(OH)C6H4, 4-(Me)C6H4, 4-(OCH3)C6H4, 4-(Cl)C6H4)

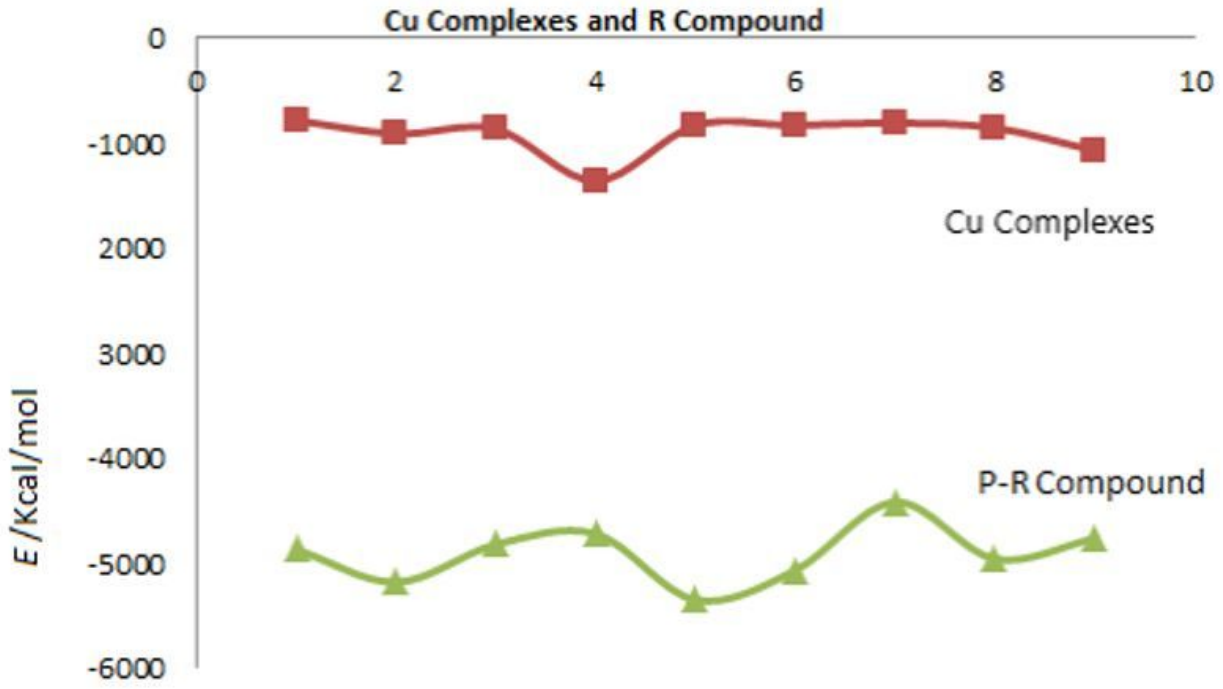

Figure 3

Energy level of pyrazoloquinolines derivatives' structure (R= Ph, 2-(NO2)C6H4, 4-(N,N-di-Me)C6H4, 2,4-di-ClC6H3, 2-(OH)C6H4, 4-(OH)C6H4, 4-(Me)C6H4, 4-(OCH3)C6H4, 4-(Cl)C6H4) and Cu complexes

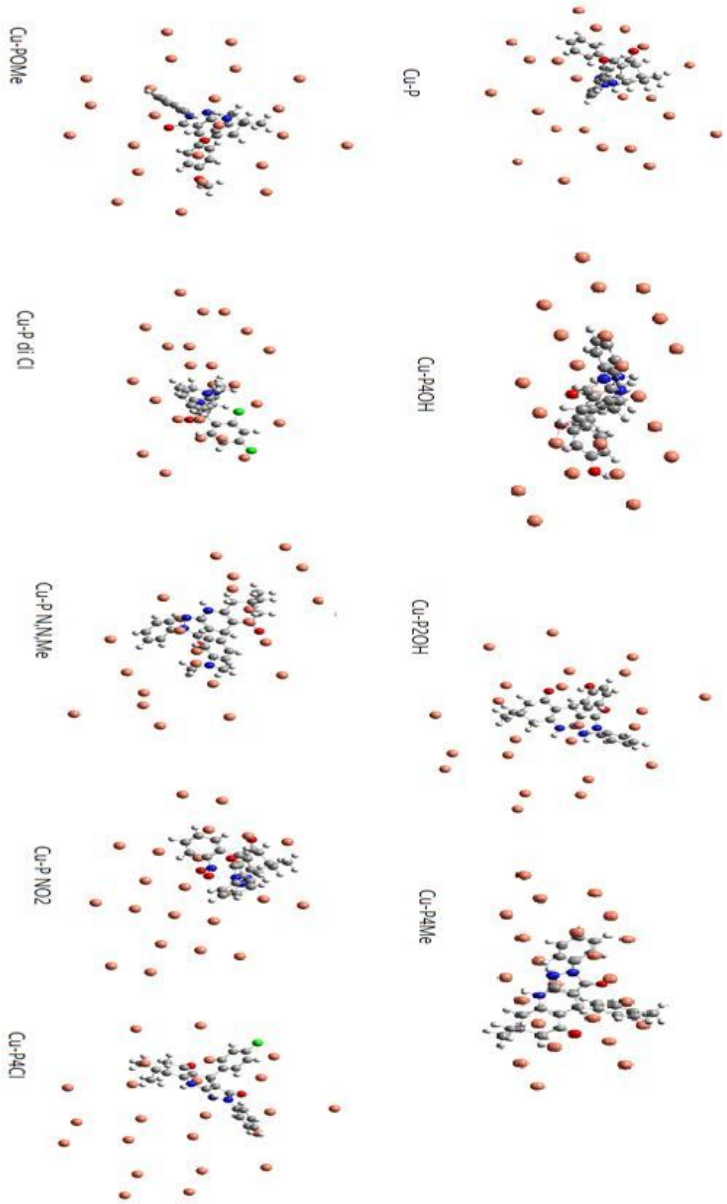

Figure 4

optimized simulated Cu-Complexes of pyrazoloquinolines derivatives

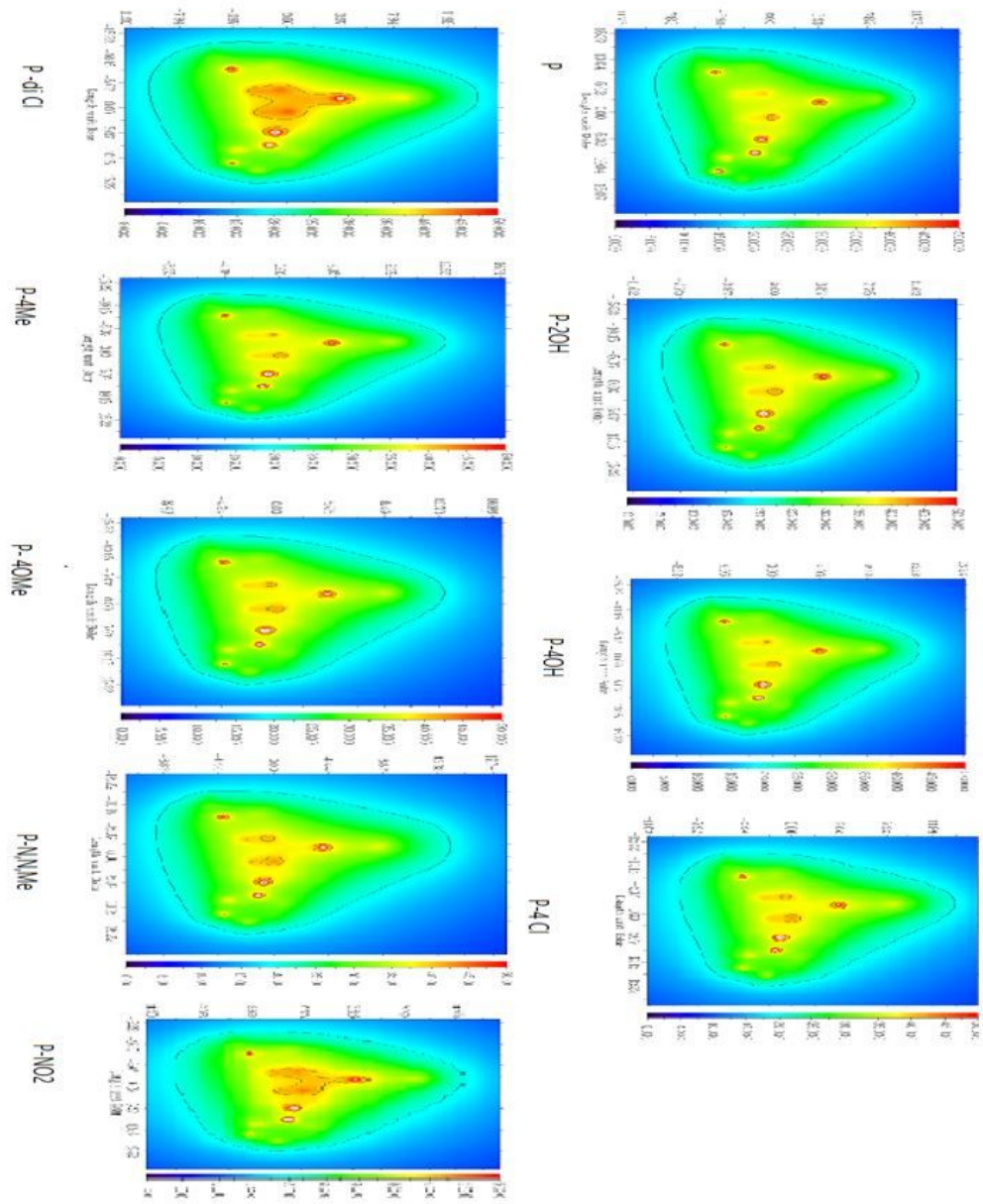

Figure 5

Electostatic potential from nuclear charges of pyrazoloquinolines derivatives contours

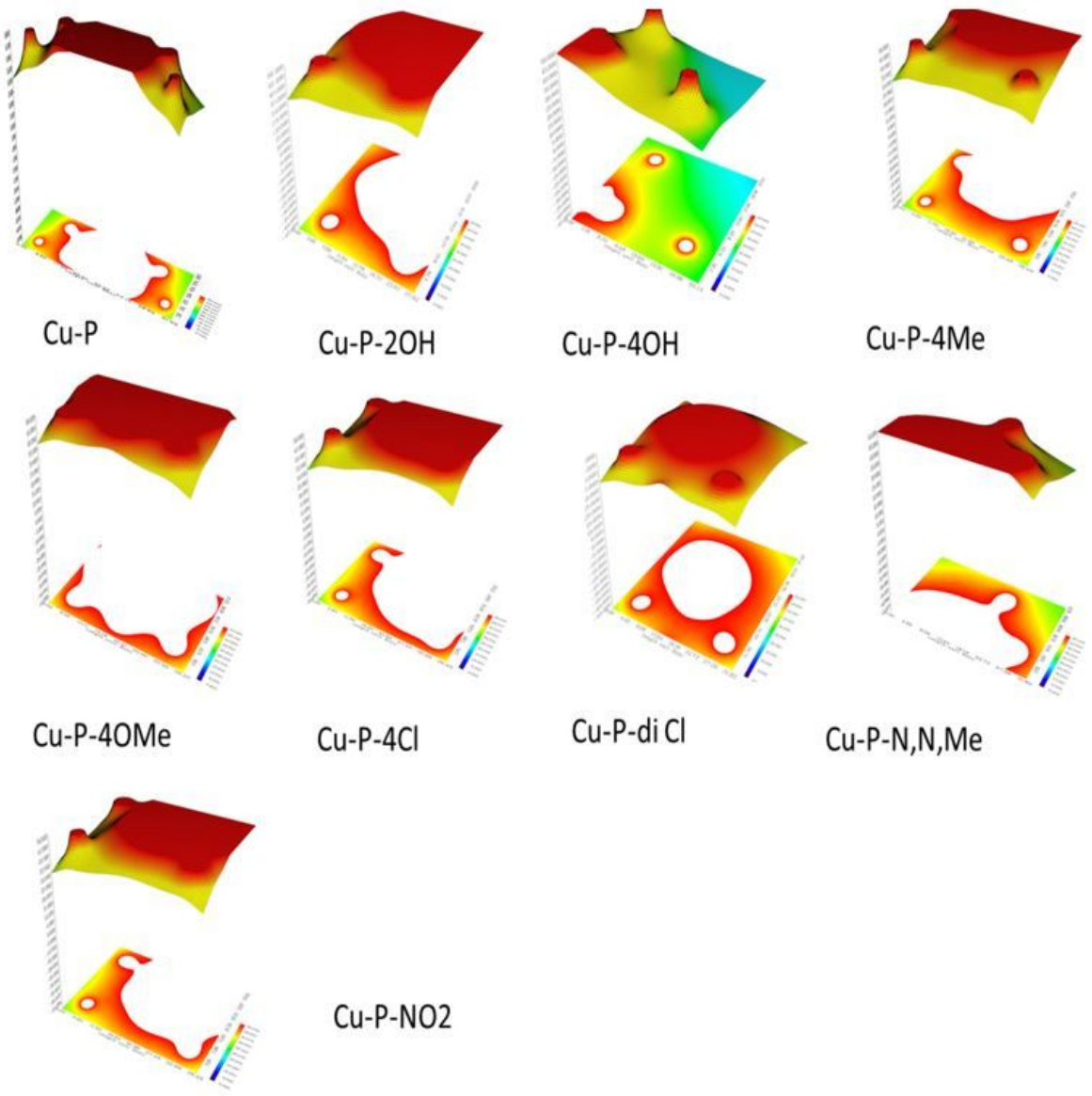

Figure 6

Electostatic potential from nuclear charges of Cu complexes of pyrazoloquinolinesderivatives profiles